

# **Gallium Oxide ( $\text{Ga}_2\text{O}_3$ ) for Power Device Application**

## **End-sem Report**

Submitted in complete fulfilment of course

### **INSTRF376 DESIGN PROJECT**

By

**Aayush Chandak – 2018B2A80433G**

**Yash Gupta - 2018B4AA0693G**

**Under the supervision of Dr. Apurba Chakraborty**



**Birla Institute of Technology And Sciences –Pilani,  
K.K. Birla Goa Campus**

## **Acknowledgement**

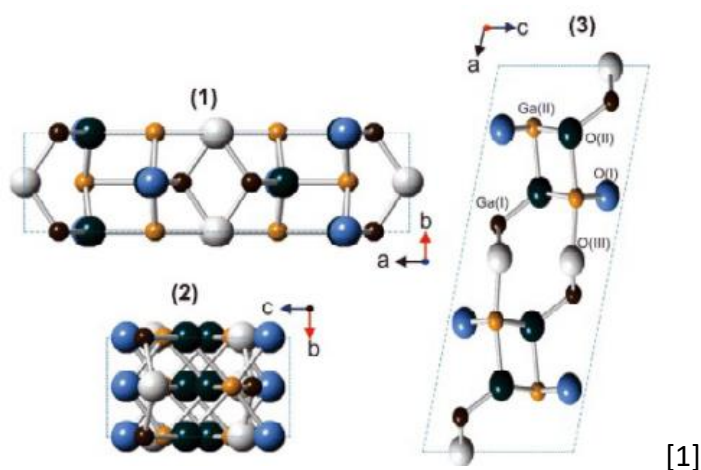
I would like to express my thankfulness to all those who have helped me and supported me during the course of the project. I would like to express my deepest gratitude to Dr. Apurba Chakraborty for giving me the opportunity to do this project and for his help and useful guidelines during the course of this project and also for helping me in writing this report.

## Table of Contents

Introduction .....	4
Literature Review .....	4
Schottky Diodes .....	5
Result and Discussion.....	6
Capacitance-Voltage characteristics model .....	6
Current-Voltage characteristics model .....	9
Figure of Merits.....	12
Baliga Figure of Merit (BFOM) .....	12
Johnson Figure of Merit (JFOM).....	13
Conclusion.....	14
References .....	15

## Introduction

The unit cell of Beta-gallium oxide ( $\beta$  -  $\text{Ga}_2\text{O}_3$ ) is shown in fig below. It contains two crystallographically inequivalent Ga positions, one with tetrahedral geometry Ga (I) and one with octahedral geometry Ga (II). The oxygen ions are arranged in a “distorted cubic” close-packed array. Oxygen atoms have three crystallographically different positions and are denoted as O(I), O(II) and O(III), respectively. Two oxygen atoms are coordinated trigonally and one is coordinated tetrahedrally.



$\beta$ - $\text{Ga}_2\text{O}_3$  is emerging as a superior semiconducting material for low frequency and high-voltage device applications owing to its ultra-wide bandgap of 4.9 eV, which is much higher than that of other wideband gap semiconductors such as GaN (3.4 eV), GaAs (1.43 eV) or 4H-SiC (2.86 eV). A larger bandgap (4.9 eV) allows  $\beta$ - $\text{Ga}_2\text{O}_3$  to withstand a stronger electric field (8 MV/cm), which makes it possible to tolerate high voltage for a given dimension of device or to use a thinner device for a given voltage. Moreover, thinner drift region provides lower specific on-resistance which permits smaller die size of the device to obtain given current capacity and thus, reduces the overall capacitance. This lower capacitance makes  $\text{Ga}_2\text{O}_3$  suitable for faster switching applications as compared to other power semiconductors.

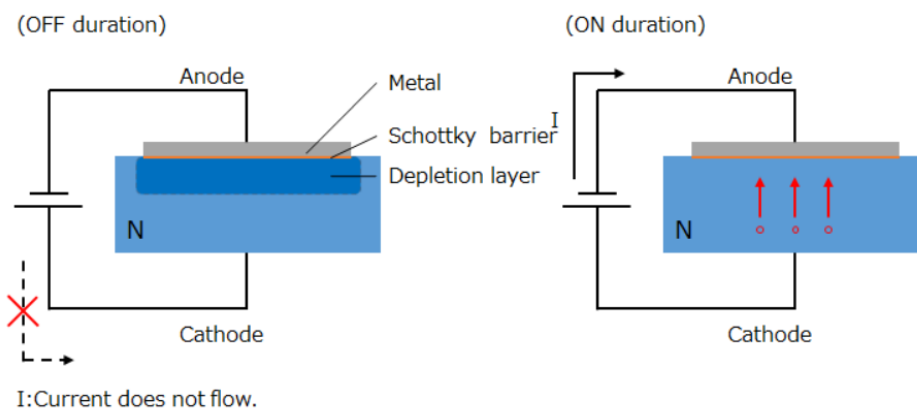
## Literature Review

Gallium oxide  $\text{Ga}_2\text{O}_3$  belongs to a family of conducting transparent semiconducting oxides (TSO). Although gallium oxide has been known for decades it remained on the periphery of the mainstream research. The history of gallium oxide dates back to 1875 when Lecoq de Boisbaudran described newly discovered element gallium and its compounds. The early publications focused on the basic research of the material as such. Later on new applications

were developed and  $\text{Ga}_2\text{O}_3$  was investigated from the stand points of microwave and optical maser studies, as a material for phosphors and electroluminescent devices, for chemical sensing and catalysis, as transparent conductive coatings etc. Gallium oxide scientific and technological research has greatly intensified over the last decade as the potential of  $\text{Ga}_2\text{O}_3$  as the perspective wide band gap semiconductor has been recognized. Purity and crystalline quality have never been a primary concern in the conventional applications of gallium oxide. On the other hand, semiconductor applications set much higher standards for the material quality and purity similar to those accepted for established semiconductors like Si or GaAs. This was a turning point in the development of  $\text{Ga}_2\text{O}_3$  research as new approaches not only opened perspectives for  $\text{Ga}_2\text{O}_3$  in semiconductor applications, but also boosted the research field as a whole.

## Schottky Diodes

Schottky barrier diodes (SBDs) are the main components of switches or rectifiers. The device performance is described by the parameters of ideality factor ( $n$ ), Schottky barrier height ( $\phi_B$ ), forward current ( $I_{\text{forward}}$ ) at specific bias, on-state resistant ( $R_{\text{on}}$ ), and reversed breakdown voltage ( $V_{\text{br}}$ ). Research on metal–semiconductor (M–S) contacts are very necessary because Schottky contacts with controllable Schottky barrier heights (SBHs) and Ohmic contacts with low series resistance are the basic requirements for achieving better device performances.



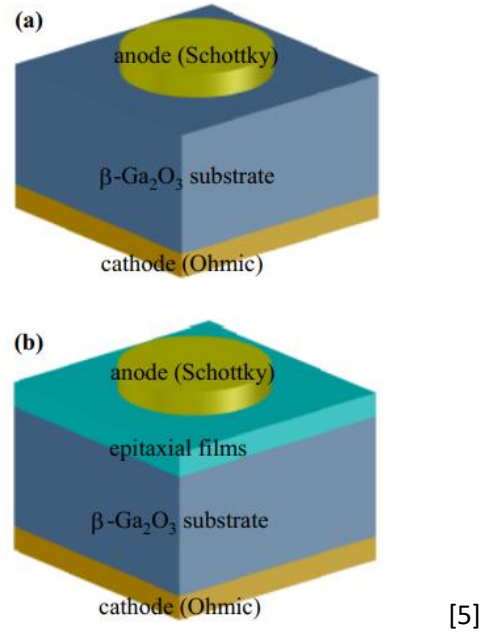
[5]

Device Operational characteristics can be described by the thermionic emission theory (TE theory), which was built by Bethe in 1942. The TE theory shows that carriers with abundant thermal energy facilitate current transport to overcome the barrier at the M–S interface.

$$I = I_0 \left[ \exp \left( \frac{qV}{nkT} - 1 \right) \right],$$

$$I_0 = AA^* T^2 \exp \left( \frac{-q\phi_B}{kT} \right), \quad [5]$$

where  $I_0$  is the reverse saturation current,  $A$  is the area of the M–S contact,  $A^*$  is the effective Richardson constant,  $V$  is the bias applied to the SBDs anode,  $n$  is the ideality factor,  $k$  is the Boltzmann constant, and  $\phi_B$  is the SBH.



## Result and Discussion

### Capacitance-Voltage characteristics model

In a schottky diode [12], the gate bias at which the channel starts to form between the source and drain is called as the threshold voltage ( $V_T$ ). A charge sheet  $n_s(x)$  is capacitively induced by the gate at the heterojunction interface when the gate voltage becomes larger than  $V_T$ . Thus,  $n_s(x)$  is negligible below  $V_T$ , hence,

$$n_s(x) \sim 0 \text{ for } V_{GS} < V_T.$$

For HFETs, channel-to-source voltage is given as

$$V_{CS}(x) = (V_{GS} - V_T) \cdot \left[ 1 - \sqrt{1 - \frac{x}{L} (1 - \alpha_s^2)} \right]$$

where  $\alpha_s$  is:

$$\alpha_s = \begin{cases} 1 - V_{DS}/(V_{GS} - V_T), & V_{DS} < (V_{GS} - V_T) \\ 0, & V_{DS} \geq (V_{GS} - V_T) \end{cases}$$

By using the formula of  $V_{CS}$  from the above in the following formula we get

$$C = \frac{Q}{[V_{GS} - V_T - V_{CS}(x)]}$$

Capacitance formula as

$$C = \frac{Q}{(V_{GS} - V_T) \cdot \sqrt{1 - \frac{x}{L} (1 - \alpha_s^2)}}$$

Where

$$\frac{x}{L} \approx \sqrt{\frac{(|V_{GS} - V_T - 0|)}{|V_{GS} - V_T - V_{CS}|}} = \sqrt{\frac{(|V_{GS} - V_T|)}{|V_{FB}|}}$$

$$\alpha_s = 1 - V_{CS}/(V_{GS} - V_T) = V_{FB}/(V_{GS} - V_T)$$

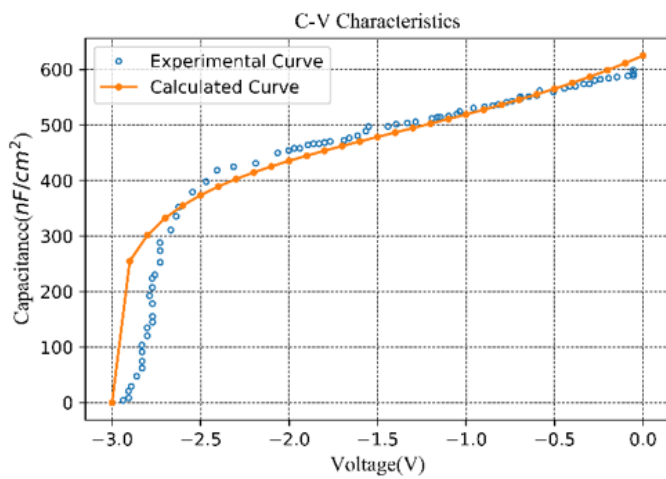
$$Q = qn_s \quad n_s(x) = n_s \sqrt{\frac{(|V_{GS} - V_T|)}{|V_{FB}|}}$$

By replacing the above quantities in the capacitance formula we get the final formula of capacitance for this model as follows:

$$C = \frac{qn_s \sqrt{\frac{(|V_{GS} - V_T|)}{|V_{FB}|}}}{(V_{GS} - V_T) \left\{ 1 - \sqrt{\frac{(|V_{GS} - V_T|)}{|V_{FB}|}} \cdot \left[ 1 - \left( \frac{|V_{FB}|}{(V_{GS} - V_T)} \right)^2 \right] \right\}^{\frac{1}{2}}}$$

By plotting this above equation for the value of  $V_{FB}^2$  such that  $6.7 \leq V_{FB}^2 \leq 8.2$  results in plots which appear similar to experimental curve with a difference of less than  $\pm 50 \text{ nF/cm}^2$  at  $V_{GS} = 0 \text{ V}$  and for  $V_{FB}^2 = 6.9$ , it matches closely to the experimental data as shown in. The flat-band voltage is estimated to be around  $-2.63 \text{ V}$ , and hence for  $V_{FB} = -2.63 \text{ V}$  (as  $V_{FB}^2 = 6.9$ ) follows the experimental curve more closely.

We have plotted the C-V characteristics by using the capacitance formula on MATLAB software for verifying the results the following plots are Fig



[1]

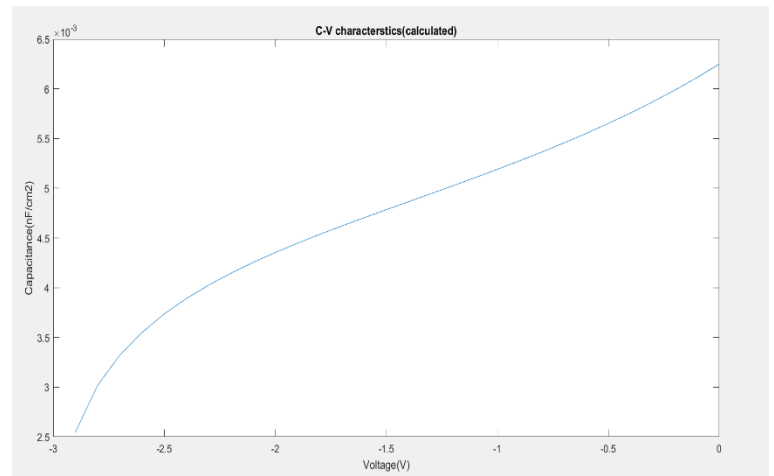


Fig. 1- C-V Characteristics(10 khz), F = 6.9 for calculated curve

Fig. 2- C-V Characteristics(10 khz), F = 6.9 for calculated curve (Matlab simulated)



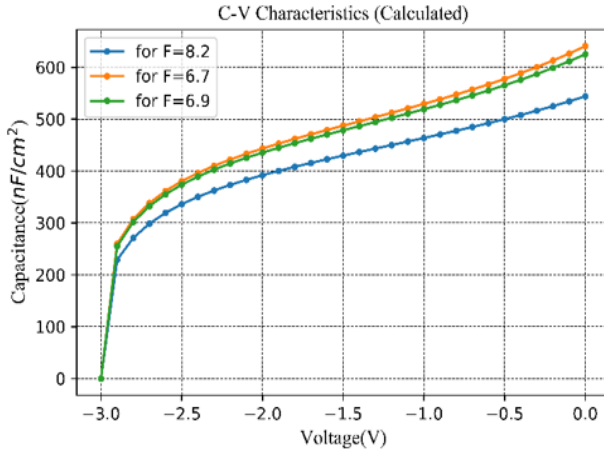


Fig. 3- C-V Characteristics for 3 different F values

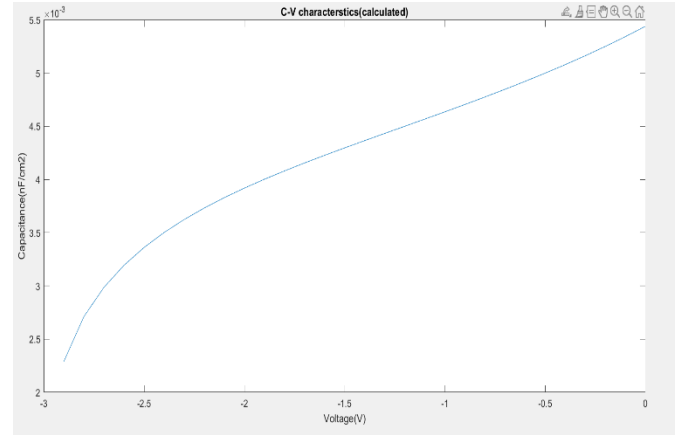


Fig. 4- C-V Characteristics for F = 8.2 (Matlab simulated )

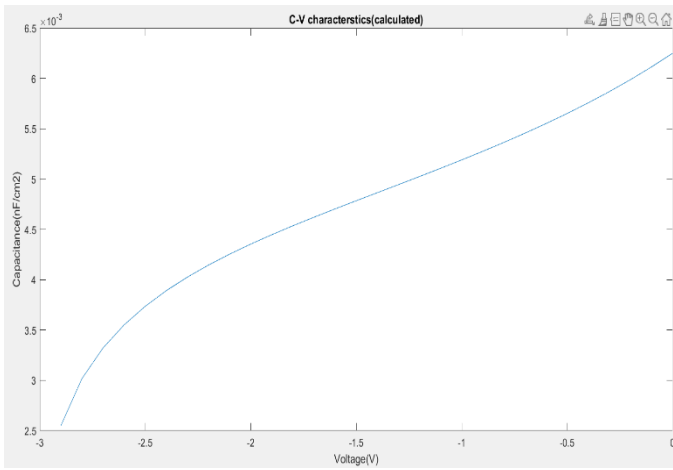


Fig. 5- C-V Characteristics for F = 6.9(Matlab simulated)

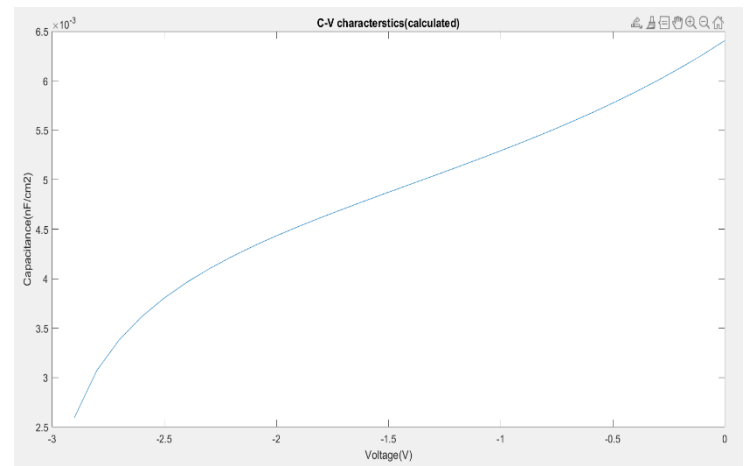


Fig. 6 – C-V Characteristics for F = 6.7 (Matlab Simulated)

## Current-Voltage characteristics model

Current in a Schottky diode is given by the following expression:

$$I = \frac{W.C.\mu.(V_{GS} - V_T)^2(1 - \alpha_s^2)}{2.L}$$

The transconductance is given by

$$g_m = \partial I / \partial V_{GS}$$

By modifying Shockley equation for FETs to fit with the experimental data, we deduce

$$I_{DS} = I_{DSS} \cdot [1 - (V_{GS}/V_p)]^{4/3}$$

From this current equation is modified to

$$I = \frac{k \cdot W \cdot C \cdot \mu \cdot (V_{GS} - V_T)^{4/3} (1 - \alpha_s^2)}{2 \cdot L}$$

The value of trans conductance ( $g_m$ ) at  $\alpha_s = 0$ ,

$$g_m = \frac{k \cdot (4/3) \cdot W \cdot C \cdot \mu \cdot (V_{GS} - V_T)^{1/3}}{2 \cdot L}$$

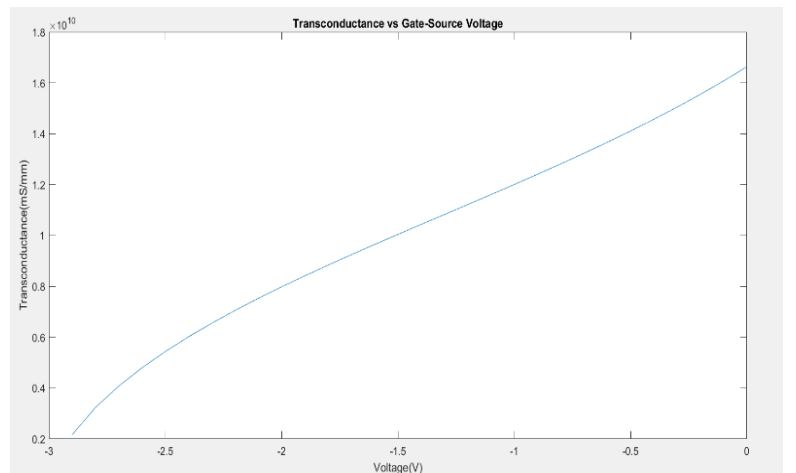
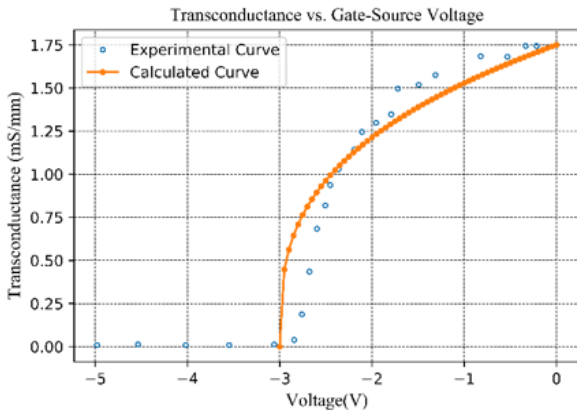
It is given that experimentally, at  $V_{GS} = 0V$ , the transconductance is 1.75 mS/mm. Moreover, based on the plot, the transconductance-voltage curve appears to follow the experimental results reasonably. It confirms further superiority of the present derived model to validate the first order non-linearity's in drain current characteristics.

Hence, denoting transconductance at  $V_{GS} = 0V$  as  $g_{m0}$ , we can write:

$$g_m = (g_{m0}) \cdot [1 - (V_{GS}/V_T)]^{1/3}$$

Where  $g_{m0}$  is given as

$$g_{m0} = \frac{k \cdot (4/3) \cdot W \cdot C \cdot \mu \cdot (-V_T)^{1/3}}{2 \cdot L}$$



[1]

Fig. 7- Trans conductance vs Voltage curve

Fig. 8 - Trans conductance vs Voltage curve (Matlab simulated)

Now from the above analysis we can write current in terms of trans conductance and the expression for the current is as follows:

$$I = \frac{(g_{m0}). [V_{GS} - V_T]^{4/3}. (1 - \alpha_s^2)}{(4/3). (-V_T)^{1/3}}$$

$$V_{DS,sat} = V_{DS,sat} (at V_{gs}=0V) - V_{GS}$$

As  $\beta$ -Ga<sub>2</sub>O<sub>3</sub> shows n-type conductivity we can say that

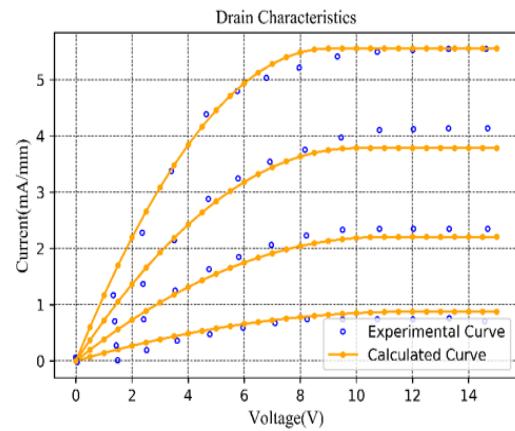
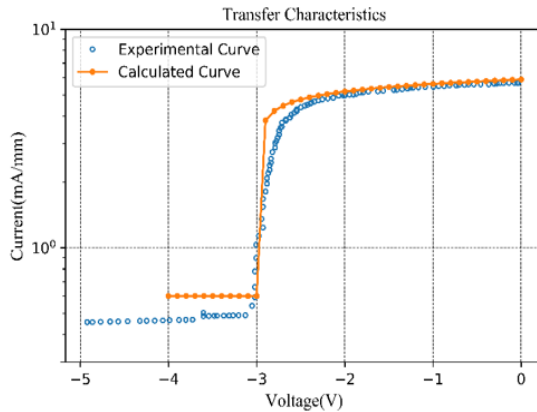
From this we have:

- When  $V_{DS} < V_{DS, saturation}$
- When  $V_{DS} \geq V_{DS, saturation}$  then  $\alpha_s = 0$

$$\alpha_s = 1 - V_{DS}/V_{DS,sat}$$

$V_{DS,sat} (at V_{gs}=0V)$  has been taken as 10 V while plotting the I-V curves.

The transfer characteristics has been plotted at  $V_{DS} = 15$  as shown in Fig. which not only validates the ability of the model to capture experimental results but also confirms higher order superiority in fitting.



[1]

Fig9. Comparison of experimental and modelled

Fig10. Drain Characteristics for  $V_{GS} = -2 \text{ V}$  to  $1 \text{ V}$  with  $\Delta V_{GS} = 1 \text{ V}$  transfer characteristics for  $V_{DS} = 15 \text{ V}$ .

The model and experimental drain characteristics are further compared and depicted in above fig. which clearly shows excellent similarity at different  $V_{GS}$  ( $-2 \text{ V}$  to  $1 \text{ V}$  with  $\Delta V_{GS}$  of  $1 \text{ V}$ ) with  $V_{DS}$  from  $0$  to  $15 \text{ V}$ .

As the model is not entirely based on physical interpretation of device inside phenomena and considers simplified empirical relations, it is named as hybrid compact model.

These models are developed by simplifying the basic device equations in different regions of operation and combining them. The modelled results exhibit good agreement with the experimental results. Thus, the model would be very useful to further optimize the heterostructure with physical insights.

## Figure of Merits

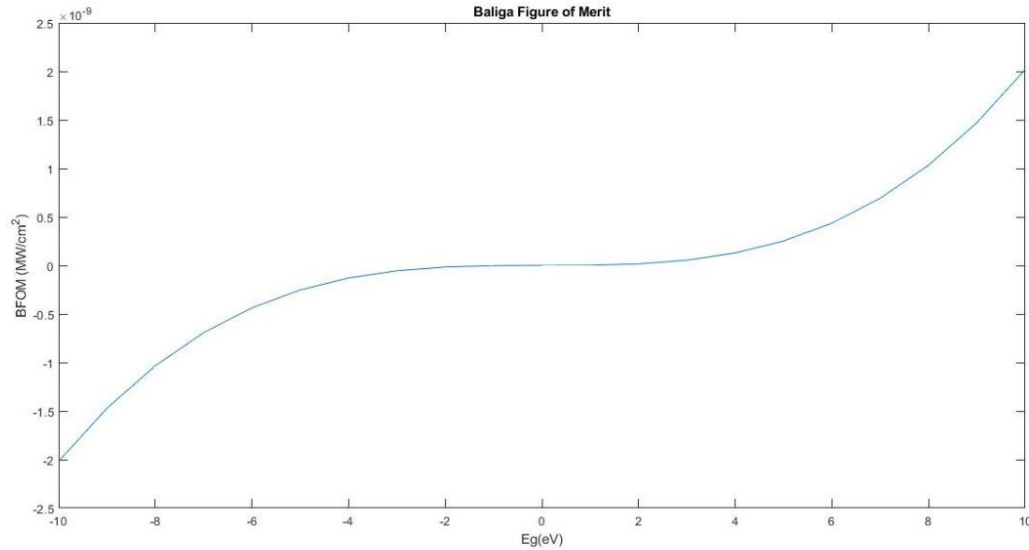
### Baliga Figure of Merit (BFOM)

Baliga figure of merit is derived for power semiconductor devices operating in high-frequency circuits. Using this figure of merit, it is predicted that the power losses incurred in the power device will increase as the square root of the operating frequency and approximately in proportion to the output power. By relating the device power dissipation to the intrinsic material parameters, it is shown that the power loss can be reduced by using semiconductors with larger mobility and critical electric field for breakdown. Examination of data in the literature indicates that significant performance improvement can be achieved by replacing silicon with gallium arsenide, silicon carbide, or semiconducting diamond.

$$BFOM = \epsilon_s \cdot \mu \cdot E_g^3$$

Where  $\epsilon_s$  is the relative permittivity for the semiconductor material and  $\mu$  is the electron mobility for the material and  $E_g$  is the breakdown voltage for the semiconductor material.

Following figure shows the variation of BFOM as the break down voltage of the material changes which helps us to interpret that which material with that break down voltage is good for our purpose.



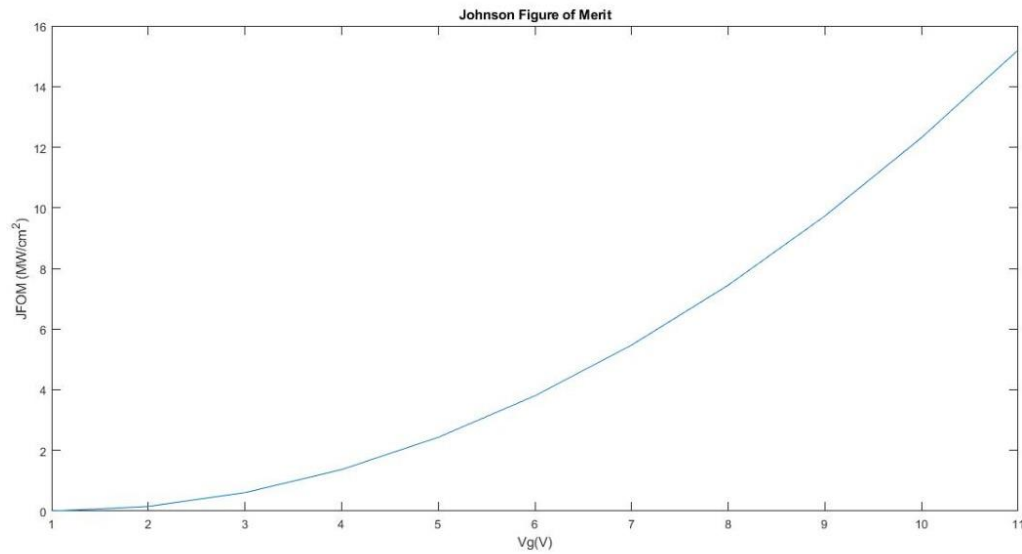
## Johnson Figure of Merit (JFOM)

Johnson's figure of merit is a measure of suitability of a semiconductor material for high frequency power transistor applications and requirements. More specifically, it is the product of the charge carrier saturation velocity in the material and the electric breakdown field under same conditions, first proposed by Edward O. Johnson of RCA in 1965.

$$\text{JFOM} = \frac{E_B^2 \cdot v_s^2}{4\pi^2}$$

Where  $E_b$  is the bandgap in the semiconductor material  $v_s$  is the voltage in the semiconductor layer.

Following curve shows the variation of JFOM with the voltage in the semiconductor material –



## Conclusion

We basically provided a compact and optimized model for the C-V and I-V characteristics of (AlGa)2O3/Ga2O3 HEMTs that includes physics-oriented analytical equations as well as reduced empirical relationships. The model is created by merging and simplifying the essential device equations in various operating zones. The simulated results are very similar to the experimental ones. Then we also analyzed the Baliga figure of merit which is a metric of potential unipolar device performance and the (AlGa)2O3/Ga2O3 HEMTs is basically having large Baliga's figure of merit (BFOM), so it is a promising candidate for the next-generation high-power devices including Schottky barrier diode (SBD). Then we analyzed the Johnson figure of merit (JFOM) which is a benchmark for RF performance and from the analysis we can say that it is able to maintain a comparable RF performance that is why it is one of the ideal choices for power devices and photodetector device applications. Thus we can conclude that these models will be really useful in making the further optimization in the heterostructure and the analysis of Baliga's figure of merit (BFOM) and the Johnson figure of merit tells us that it is a promising candidate for the power devices and photo detector applications.

## References

1. S. Krishnamoorthy, Z. Xia, C. Joishi, Y. Zhang, J. McGlone, J. Johnson, M. Brenner, A. R. Arehart, J. Hwang, S. Lodha, and S. Rajan, "Modulation-doped  $\beta$ - ( $\text{Al}_{0.2}\text{Ga}_{0.8}$ ) $_2\text{O}_3/\text{Ga}_2\text{O}_3$  field-effect transistor," Appl. Phys. Lett., vol. 111, 023502, pp. 3–7, 2017.
2. S. Stepanov, V. Nikolaev, V. Bougrov and A. Romanov "Gallium oxide: properties and applications- a review," Rev. Adv. Mater. Sci. 44 (2016) 63-86 [http://www.ipme.ru/e-journals/RAMS/no\\_14416/06\\_14416\\_stepanov.pdf](http://www.ipme.ru/e-journals/RAMS/no_14416/06_14416_stepanov.pdf)
3. Zeng Liu, Zhi Yusong, Wang Xiaolong - Review of gallium oxide based field-effect transistors and Schottky barrier diodes.
4. <https://iopscience.iop.org/article/10.1088/0268-1242/31/3/034001#ssta0f2as4>
5. <https://nanoscalereslett.springeropen.com/articles/10.1186/s11671-018-2712-1>
6. [https://www.researchgate.net/publication/284187933\\_Near\\_valence-band\\_electronic\\_properties\\_of\\_semiconducting\\_b-Ga2O3\\_100\\_single\\_crystals/figures?lo=1&utm\\_source=google&utm\\_medium=organic](https://www.researchgate.net/publication/284187933_Near_valence-band_electronic_properties_of_semiconducting_b-Ga2O3_100_single_crystals/figures?lo=1&utm_source=google&utm_medium=organic)
7. [https://en.wikipedia.org/wiki/Johnson%27s\\_figure\\_of\\_merit](https://en.wikipedia.org/wiki/Johnson%27s_figure_of_merit)